# Structure and bonding in redox-active d$^4$, d$^5$ and d$^6$ alkyne complexes: metal–alkyne moieties as electron sinks

**Ian M. Bartlett, Neil G. Connelly,* A. Guy Orpen,* Michael J. Quayle and James C. Rankin**

*School of Chemistry, University of Bristol, Bristol, UK BS8 1TS*

**X-Ray structural studies of the two redox-related pairs [Cr(CO)$_2$(η-PhC≡CPh)(η$^6$-C$_6$HMe$_5$)]$^{0/1+}$ and [Mo(CO)$_2$(η-Ph≡CPh)(Tp′)]$^{0/1+}$ [Tp′ = hydrotris(3,5-dimethylpyrazolyl)borate] are consistent with the HOMO of the d$^6$, Cr$^0$ alkyne complex being an antibonding M–alkyne π$_\perp$ orbital.**

Because an alkyne can bind to a transition metal as a net two-, three- or four-electron donor, for example in [Cr(CO)$_2$(η-PhC≡CPh)(η-C$_6$Me$_6$)],[1] [Mo(NCMe)(η-MeC≡CMe)$_2$(η-C$_5$H$_5$)]$^{+2}$ and [W(CO)$_2$(η-PhC≡CPh)(Tp′)]$^+$ [Tp′ = HB(3,5-dimethylpyrazolyl)$_3$][3] respectively, one might expect the different bonding modes to be interconvertible by one-electron-transfer reactions. Certain alkyne complexes are, indeed, redox-active, and redox-related pairs of the type [Cr(CO)$_2$(alkyne)(η-arene)]$^{z+}$ ($z$ = 0, 1), for example, have been spectroscopically characterised.[4] We now describe the structural characterisation of two such pairs, namely [Cr(CO)$_2$(η-PhC≡CPh)(η-C$_6$HMe$_5$)] and [Cr(CO)$_2$(η-PhC≡CPh)(η-C$_6$HMe$_5$)]PF$_6$, and [Mo(CO)$_2$(η-PhC≡CPh)(Tp′)] and [Mo(CO)$_2$(η-PhC≡CPh)(Tp′)]PF$_6$ which provides detailed insight into the effects of electron transfer on alkyne–metal bonding. The structural changes observed on electron transfer are consistent with the HOMO in d$^6$ [ML$_5$(η-alkyne)] complexes being an antibonding M–alkyne π$_\perp$ orbital.

Treatment of [Cr(CO)$_2$(η-PhC≡CPh)(η-C$_6$HMe$_5$)] **1** in CH$_2$Cl$_2$ with [Fe(η-C$_5$H$_5$)$_2$]PF$_6$ gives [Cr(CO)$_2$(η-PhC≡CPh)(η-C$_6$HMe$_5$)]PF$_6$, **1**$^+$PF$_6$$^-$;[5] crystals of its dichloromethane solvate were grown from *n*-hexane–CH$_2$Cl$_2$. The molecular structures of **1** (grown from *n*-hexane–acetone) and **1**$^+$ were determined; that of the cation is shown in Fig. 1 with important bond lengths and angles for both given in Table 1.

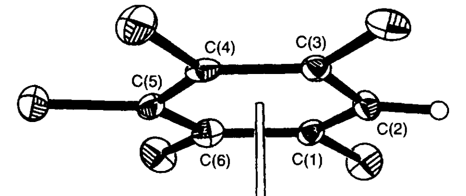

**Fig. 1** Structure of **1**$^+$ (hydrogen atoms omitted for clarity); important bond lengths and angles are given in Table 1

The cationic four-electron alkyne complexes [W(CO)$_2$(η-RC≡CR)(Tp′)]PF$_6$ [Tp′ = HB(3,5-dimethylpyrazolyl)$_3$] are well known[3] and the molybdenum analogue [Mo(CO)$_2$(η-PhC≡CPh)(Tp′)]PF$_6$, **2**$^+$PF$_6$$^-$ can be prepared similarly, *i.e.* by the addition of [Fe(η-C$_5$H$_5$)$_2$]PF$_6$ to a mixture of [Mo-(CO)$_3$(Tp′)][6] and PhC$_2$Ph in CH$_2$Cl$_2$.† Surprisingly, the redox chemistry of the cationic alkyne complexes has not been previously reported. The cyclic voltammogram of **2**$^+$PF$_6$$^-$ in CH$_2$Cl$_2$ shows a reversible reduction wave at −0.10 V (a second incompletely reversible wave is also observed at −1.33 V) and treatment of **2**$^+$PF$_6$$^-$ with [Co(η-C$_5$H$_5$)$_2$] in CH$_2$Cl$_2$ gave† green–black crystals of [Mo(CO)$_2$(η-PhC≡CPh)(Tp′)] **2**. The structures of **2**·0.5 C$_6$H$_{14}$ and **2**$^+$PF$_6$$^-$ (crystals of which were grown from hot *n*-hexane and *n*-hexane–CH$_2$Cl$_2$ respectively) were determined; that of the neutral molecule **2** is shown in Fig. 2 with important bond lengths and angles for both given in Table 1. {As might be expected, the structural parameters of **2**$^+$ are rather similar to those of the tungsten complex [W(CO)$_2$(η-PhC≡CMe)(Tp′)]$^+$.[7]}

A comparison within each redox-related pair shows that the major change observed on oxidation is a shortening of the M–C$_{\text{alkyne}}$ bonds (by *ca.* 0.11 and 0.10 Å for **1** and **2** respectively). For **2** there is a corresponding lengthening of the C≡C bond (by *ca.* 0.05 Å) though a similar change is not detectable on oxidation of **1**. These structural changes are in sharp contrast to those observed on oxidation of a metal–alkene complex. Thus, on oxidising[8] [Mo$_2$(μ-C$_8$Me$_8$)(η-C$_5$H$_5$)$_2$] to [Mo$_2$(μ-C$_8$Me$_8$)(η-C$_5$H$_5$)$_2$]$^+$ the lengthening of Mo–C and the shortening of C=C in the Mo(alkene) fragment is consistent with the Dewar–Chatt–Duncanson model for metal–alkene bonding; the electron is removed from an orbital formed by the overlap of a filled metal orbital and the π* alkene orbital.

Because of the second C–C π-bond (π$_\perp$) present, metal–alkyne bonding is potentially more complex than metal–alkene bonding.[4,9–12] In a pseudo-octahedral d$^6$ [ML$_5$(η-alkyne)] species (such as **1** in which the η-C$_6$Me$_5$H ligand acts as a six-

**Table 1** Bond lengths (Å) and angles (°) for alkyne complexes

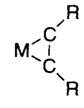

| Complex | Metal electron configuration | M–C | C–C | R–C–C |
|---|---|---|---|---|
| 1 | d$^6$ | 2.144(2)<br>2.136(2) | 1.259(2) | 150.3(2)<br>149.1(2) |
| 1$^+$ | d$^5$ | 2.044(7)<br>2.032(6) | 1.260(10) | 144.8(6)<br>146.3(6) |
| 2 | d$^5$ | 2.136(3)<br>2.175(3) | 1.282(3) | 140.7(2)<br>143.7(2) |
| 2$^+$ | d$^4$ | 2.041(4)<br>2.069(3) | 1.334(6) | 141.3(3)<br>142.6(4) |

electron donor $L_3$ set) the HOMO is the antibonding M–alkyne $\pi_\perp$ orbital illustrated in Fig. 3. This orbital arises by out-of-phase overlap of one of the $t_{2g}$-like metal orbitals with the filled alkyne $\pi_\perp$ orbital. (The bonding combination of these orbitals is of course filled for any occupancy of the $t_{2g}$ set.) However, for $d^5$ (as in $\mathbf{1}^+$ and **2**) and $d^4$ (as in $\mathbf{2}^+$) configurations the antibonding orbital is successively depopulated and the M–alkyne bond order increases, and hence the M–$C_{alkyne}$ bonds shorten on oxidation. Somewhat similar structural effects have been observed[13] for the $d^8$ [$ML_3$(η-alkyne)] and $d^8$ [$ML_4$(η-alkyne)] complexes [Co($PMe_3$)$_3$(η-PhC≡CPh)]$^+$ and [Co($PMe_3$)$_3$(NCMe)(η-PhC≡CPh)]$^+$ where nitrile coordination converts a four-electron alkyne to a two-electron alkyne, and the Co–C bond lengths increase by *ca.* 0.13 Å.

The appearance of a $^1H$ coupling in the EPR spectrum of [Cr(CO)$_2$(η-HC≡CPh)(η-$C_6Me_6$)]$^+$ suggests significant delocalisation of spin on to the alkyne in $d^5$ [$ML_5$(η-alkyne)] complexes.[4] However, it is clear from the molecular orbital analysis that the contribution of the metal to the SOMO in the $d^5$ alkyne complexes will vary; in part the relative energies of the relevant metal $t_{2g}$ orbital (which will depend on the ligand set and the metal itself) and the alkyne $\pi_\perp$ orbital will determine the characteristics of the resultant SOMO. The isolation of the two redox-related pairs **1**/$\mathbf{1}^+$ and **2**/$\mathbf{2}^+$ shows that the metal–alkyne moiety may act as an electron sink, allowing formation of stable complexes with formal $d^4$, $d^5$ or $d^6$ configurations which may be interconverted by electron-transfer reactions.

We thank the EPSRC for a studentship (to M. J. Q.) and the University of Bristol for a postgraduate scholarship (to I. M. B.).

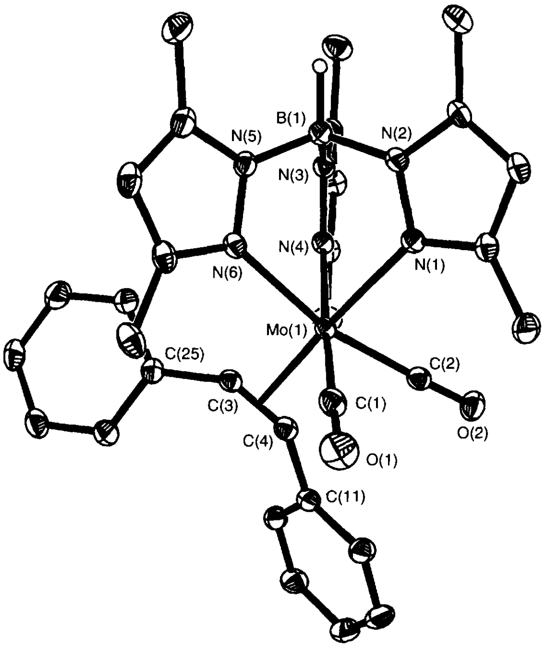

**Fig. 2** Structure of **2** (hydrogen atoms omitted for clarity); important bond lengths and angles are given in Table 1

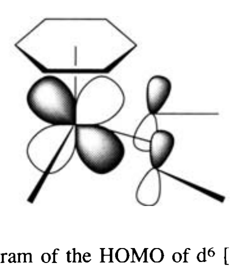

**Fig. 3** Schematic diagram of the HOMO of $d^6$ [$ML_2$(η-alkyne)(η-$C_6H_6$)] complexes such as **1**

## Footnotes

† All new complexes had satisfactory elemental analyses (C and H). Complex $\mathbf{1}^+PF_6^-\cdot CH_2Cl_2$: red crystals, yield 62%; IR: ν(CO)($CH_2Cl_2$) 2065 and 2002 cm$^{-1}$; $^1H$ NMR ($CD_2Cl_2$): δ 8.36–7.15 (m, 10 H, Ph), 6.15 (s, 1 H, $C_3N_2\mathit{H}Me_2$), 5.87 (s, 2 H, $C_3N_2\mathit{H}Me_2$), 2.82, (s, 3 H, $C_3N_2H\mathit{Me}_2$), 2.66, (s, 6 H, $C_3N_2HMe_2$), 2.52 (s, 3 H, $C_3N_2H\mathit{Me}_2$), 1.12 (s, 3 H, $C_3N_2H\mathit{Me}_2$). Complex **1**: green–black crystals, yield 48%; IR: ν(CO)($CH_2Cl_2$) 1962 and 1876 cm$^{-1}$; EPR (toluene), 300 K, $g_{iso}$ = 2.007, $A(^{95,97}Mo)$ = 30.7G; 77 K, $g_1$ = 2.036, $g_2$ = 2.009, $g_3$ = 1.977, $g_{av}$ = 2.007.

§ *Crystal data*: [Cr(CO)$_2$(η-PhC≡CPh)(η-$C_6HMe_5$)] **1**: $C_{27}H_{26}CrO_2$, $M$ = 434.48, triclinic, space group $P\bar{1}$ (no. 2), $a$ = 7.1132(14), $b$ = 9.353(3), $c$ = 16.781(3) Å, α = 88.5(2), β = 81.8(2), γ = 71.9(2)°, $U$ = 1050.6(4) Å$^3$, $Z$ = 2, $D_c$ = 1.373 Mg m$^{-3}$, $\bar{\lambda}$ = 0.71 073 Å, μ = 0.566 mm$^{-1}$, $F(000)$ = 456, $T$ = 173 K. Data (4987 total, 3518 unique, $R_{int}$ = 0.021) were collected on a Siemens SMART diffractometer for a full hemisphere of reciprocal space with $2 < \theta < 25°$. The structure was solved by direct methods and refined by least squares against all 3517 $F^2$ values with $F^2 > -3\sigma(F^2)$ corrected for absorption to $wR2$ = 0.077 [$R1$ = 0.028 for 3332 data with $F^2 > 2\sigma(F^2)$].

[Cr(CO)$_2$(η-PhC≡CPh)(η-$C_6HMe_5$)]$PF_6\cdot CH_2Cl_2$, $\mathbf{1}^+PF_6^-\cdot CH_2Cl_2$: $C_{28}H_{28}Cl_2CrF_6O_2P$, $M$ = 664.37, monoclinic, space group $P2_1$ (no. 4), $a$ = 9.187(2), $b$ = 15.768(3), $c$ = 9.913(3) Å, β = 100.89(2)°, $U$ = 1410.4(5) Å$^3$, $Z$ = 2, $D_c$ = 1.564 Mg m$^{-3}$, $\bar{\lambda}$ = 0.71073 Å, μ = 0.717 mm$^{-1}$, $F(000)$ = 678, $T$ = 173 K. Data (6858 total, 3808 unique, $R_{int}$ = 0.054) were collected and analysed as for **1**. For all 3807 $F^2$ values with $F^2 > -3\sigma(F^2)$, $wR2$ = 0.121 [$R1$ = 0.054 for 3243 data with $F^2 > 2\sigma(F^2)$].

[Mo(CO)$_2$(η-PhC≡CPh)(Tp′)]·0.5$C_6H_{14}$, **2**·0.5$C_6H_{14}$: $C_{34}H_{39}BMoN_6O_2$, $M$ = 670.46, monoclinic, space group $P2_1/n$ (no. 14), $a$ = 10.124(2), $b$ = 15.0985(13), $c$ = 21.857(2) Å, β = 101.90(9)°, $U$ = 3269.3(7) Å$^3$, $Z$ = 4, $D_c$ = 1.362 Mg m$^{-3}$, $\bar{\lambda}$ = 0.71073 Å, μ = 0.441 mm$^{-1}$, $F(000)$ = 1392, $T$ = 173 K. Data (15 197 total, 5707 unique, $R_{int}$ = 0.026) were collected and analysed as for **1**. For all 5707 $F^2$ values with $F^2 > -3\sigma(F^2)$, $wR2$ = 0.078 [$R1$ = 0.029 for 5206 data with $F^2 > 2\sigma(F^2)$].

[Mo(CO)$_2$(η-PhC≡CPh)(Tp′)]$PF_6$, $\mathbf{2}^+\cdot PF_6^-$: $C_{31}H_{32}BF_6MoN_6O_2P$, $M$ = 772.35, orthorhombic, space group $P2_12_12_1$ (no. 19), $a$ = 14.7387(11), $b$ = 14.8580(14), $c$ = 15.554(2) Å, $U$ = 3406.2(6) Å$^3$, $Z$ = 4, $D_c$ = 1.506 Mg m$^{-3}$, $\bar{\lambda}$ = 0.71073 Å, μ = 1.437 mm$^{-1}$, $F(000)$ = 1568, $T$ = 173 K. Data (16 071 total, 5972 unique, $R_{int}$ = 0.0484) were collected and analysed as for **1**. For all unique $F^2$ values $wR2$ = 0.096 [$R1$ = 0.037 for 5742 data with $F^2 > 2\sigma(F^2)$]. Atomic coordinates, bond lengths and angles, and thermal parameters have been deposited at the Cambridge Crystallographic Data Centre (CCDC). See Information for Authors, Issue No. 1. Any request to the CCDC for this material should quote the full literature citation and the reference number 182/272.

## References

1 W. Strohmeier and H. Hellmann, *Chem. Ber.*, 1965, **98**, 1598.
2 M. Green, *Polyhedron*, 1986, **5**, 427.
3 S. G. Feng, C. C. Philipp, A. S. Gamble, P. S. White and J. L. Templeton, *Organometallics*, 1991, **10**, 3504.
4 N. G. Connelly, A. G. Orpen, A. L. Rieger, P. H. Rieger, C. J. Scott and G. M. Rosair, *J. Chem. Soc., Chem. Commun.*, 1992, 1293.
5 N. G. Connelly and G. A. Johnson, *J. Organomet. Chem.*, 1974, **77**, 341.
6 K.-B. Shiu and L.-Y. Lee, *J. Organomet. Chem.*, 1988, **348**, 357.
7 J. L. Templeton, J. L. Caldarelli, S. Feng, C. C. Philipp, M. B. Wells, B. E. Woodworth and P. S. White, *J. Organomet. Chem.*, 1994, **478**, 103.
8 N. G. Connelly, B. Metz, A. G. Orpen and P. H. Rieger, *Organometallics*, 1996, **15**, 729.
9 B. E. R. Schilling, R. Hoffmann and D. L. Lichtenberger, *J. Am. Chem. Soc.*, 1979, **101**, 585.
10 S. R. Allen, R. G. Beevor, M. Green, N. C. Norman, A. G. Orpen and I. D. Williams, *J. Chem. Soc., Dalton Trans.*, 1985, 435.
11 D. C. Brower, K. R. Birdwhistell and J. L. Templeton, *Organometallics*, 1986, **5**, 94 and references therein.
12 K. R. Birdwhistell, T. L. Tonker and J. L. Templeton, *J. Am. Chem. Soc.*, 1987, **109**, 1401.
13 B. Capelle, M. Dartiguenave, Y. Dartiguenave and A. L. Beauchamp, *J. Am. Chem. Soc.*, 1983, **105**, 4662.

*Received, 12th August 1996; Com. 6/05632F*